Journal of Environmental Chemical Engineering 11 (2023) 109903

Contents lists available at ScienceDirect

Journal of Environmental Chemical Engineering

journal homepage: www.elsevier.com/locate/jece

Cathodic reduction of CO_2 to formic acid: Effect of the nature of the cathode for pressurized systems

Federica Proietto [a], Riccardo Rinicella [a], Alessandro Galia [a], Beatriz Ávila-Bolívar [b], Vicente Montiel [b], José Solla-Gullón [b], Onofrio Scialdone [a,*]

[a] Dipartimento di Ingegneria, Università degli Studi di Palermo, Viale delle Scienze, 90128 Palermo, Italy
[b] Institute of Electrochemistry, University of Alicante, Apdo. 99, Alicante E-03080, Spain

ARTICLE INFO

Editor: Despo Kassinos

Keywords:
CO_2 reduction
Formic acid
Pressure
Tin
Bismuth
Electrochemistry

ABSTRACT

Electrochemical conversion of CO_2 into formic acid (FA) in an aqueous electrolyte is considered a promising strategy to valorise waste-CO_2. Some studies, mainly performed using Sn cathodes, have shown that the performance of the process can be strongly improved using pressurized systems. On the other hand, other studies, usually carried out in non-pressurized systems, have indicated that the nature of the cathode can strongly affect the process. Hence, in this work, we have investigated the coupled effect of nature of the cathode and CO_2 pressure (P_{CO_2}) on the electrochemical conversion of CO_2 to FA. Four electrodes (Sn, Sn/C-NP, Bi, Bi/C-NP) have been used as model cathodes. The results obtained have shown that the increase of P_{CO_2} enhances the production of FA and the faradic efficiency of the process (FE_{FA}) for all tested cathodes. Moreover, it has been observed that nanoparticle-based cathodes provided better results for electrolyses carried out at 1 bar and high current density. Conversely, at relatively high P_{CO_2}, the effect of the nature of the cathode becomes less important and bulk Sn and Bi electrodes display very interesting results in terms of production of FA, FE_{FA} and stability.

1. Introduction

A promising route to valorise waste-CO_2 is its cathodic reduction (CO_2EC-CO_2 electrochemical conversion) into various chemicals [1–6]. As described in the literature, CO_2EC presents various advantages [2,7,8] including:

- the possibility to operate under mild conditions (i.e., low temperature and pressures between 1 and 30 bar);
- the production of different compounds in water, such as formic acid (FA), carbon monoxide, syngas, ethylene, etc…, by a suitable selection of operative parameters [1];
- easy scale-up and potential utilization of excess electric energy from intermittent renewable sources, available at a low price, as chemical energy, without any additional fossil fuel-based electricity, thus reducing the process' costs [8].

Moreover, the utilization of non-aqueous systems can allow using CO_2 for the electrochemical production of carboxylic acids by the addition of proper precursors, such as benzylic halides or aromatic ketones [9,10].

It has been reported that, in aqueous solvents, simple products, such as CO and FA, are likely to be more interesting from an economic point of view due to the low number of electrons ($z = 2$) required for their synthesis and to the interesting performance of adopted electrocatalysts, although only lab-scale and small pilot plant electrolyser systems have been used [7,8,11]. Indeed, CO and FA show the highest product value per electron [11]. Furthermore, for these products, relatively high faradic efficiencies (FE) and current densities (j) have been reported. Moreover, the synthesis of FA by CO_2EC process is likely to present a smaller environmental impact than conventional industrial processes [8] and the economics can become more interesting by coupling the cathodic process with a suitable anodic one (such as the wastewater treatment or the synthesis of Cl_2 [12,13]) or with an Assisted Reverse Electrodialysis process [14].

It has been shown that the performance of CO_2EC to FA can be improved by various approaches, including the utilization of gas diffusion electrodes [15–30], pressurized systems [31–40] or electrocatalytic materials with high electrode surface, activity, and selectivity [4]. However, the effect of the nature of the cathode has been usually

* Corresponding author.
E-mail address: onofrio.scialdone@unipa.it (O. Scialdone).

https://doi.org/10.1016/j.jece.2023.109903
Received 27 February 2023; Received in revised form 7 April 2023; Accepted 11 April 2023
Available online 12 April 2023

Nomenclature

Bi	Bi rod
Bi/C-NP	carbon-supported bismuth nanoparticle
$c^b_{CO_2}$	bulk CO_2 concentration (mM)
CO_2EC	CO_2 electrochemical conversion
$\mathscr{D}_{CO_2}$	CO_2 diffusion coefficient ($m^2\ s^{-1}$)
δ	thickness of the stagnant layer (μm)
ΔV	cell potential (V)
EC	energy consumption (kWh mol^{-1})
EE	energy efficiency (%)
E_{eq}	thermodynamic equilibrium cell potential (V)
F	Faraday constant (C mol^{-1})
FA	formic acid
FE	faradaic efficiency (%)
FE_{FA}	faradaic efficiency of formic acid (%)
I	current intensity (A)
j	current density (mA cm^{-2})
j_{lim}	limiting current density (mA cm^{-2})
P_{CO_2}	CO_2 pressure (bar)
Sn	tin plate
Sn/C-NP	carbon-supported tin nanoparticle
t	time (s)
T	temperature (°C)
V (L)	volume of solution (L)
z	number of electrons
[FA]	formic acid concentration (mM)

evaluated for systems operating at CO_2 pressure (P_{CO_2}) close to 1 bar and few data are available for pressurized cells. Conversely, in most cases, the studies on the effect of the P_{CO_2} on the CO_2EC to FA have been performed only using Sn-based cathodes.

Hence, in this work, we have performed a detailed analysis of the effect of the nature of the cathode at various P_{CO_2} and j on the CO_2EC process performances into FA. Four electrode materials have been selected as model cathodes based on the state of the art:

- Tin plate (Sn) and *ii*) carbon-supported tin nanoparticle (Sn/C-NP)

Sn electrocatalysts have been the most extensively investigated cathodes for the electrochemical synthesis of FA since 1976 [42] thanks to their high catalytic activity and selectivity towards FA/formate (>90%) in aqueous electrolytes. Several studies have shown that the Sn plate is an active form and the most stable form among the Sn-based catalysts reported in the literature [35,36,43]. Proietto et al. [36] showed that the concentration of FA ([FA]) as high as 0.38 M coupled with a good FE after more than 40 h were achieved using a Sn plate under pressurized conditions. Recently, several strategies have been used to tune the performance of Sn electrocatalysts. As an example, these metals are usually deposited in form of particles to maximize the active surface with the minimum amount of metal and recent studies have shown that the structure and size of these particles have a great influence on the selectivity and behaviour of the electrochemical reduction. Del Castillo et al. [30,31] have shown that the usage of Sn/C-NP allows to achieve a FE of formate of 70% coupled with a concentration of 54 mM at 150 mA cm^{-2} in a divided filter-press type cell equipped with a Sn-GDE. In addition, they have demonstrated that metal loading and particle size play a relevant role in the performance of CO_2 reduction: smaller Sn nanoparticles displayed higher selectivity. Furthermore, according to the literature, to date, only for Sn-based cathodes there is an interesting engineering and economic feasibility to produce FA on the large-scale, thanks to its non-noble, eco-friendly, and low-cost characteristics [8].

- *iii*) Bismuth (Bi) and *iv*) carbon-supported bismuth nanoparticle (Bi/C-NP)

The electrochemical CO_2EC performances using Bi were first reported by Komatsu in 1995 [44]. More recently, Bi has aroused great interest as an electrocatalyst for producing FA/formate at lower overpotentials with respect to the other metal-based cathodes [29,45–48]. Bi-electrocatalysts are also characterized by low toxicity, low cost, and high stability under electrochemical conditions in aqueous media. In addition, the H_2 evolution reaction (HER) is poorly electro-catalyzed by Bi due to its positive free energy of hydrogen adsorption. Su et al. [48] reported that FE towards formate as high as 85% was achieved using commercial Bi at − 0.9 V vs RHE in a divided conventional cell. Recently, Bi/C-NP was simply synthesized and tested as cathodes for the synthesis of FA. Ávila-Bolívar et al. [47] showed that the usage of Bi/C-NP electrocatalysts allows reaching a FE of FA up to approximately 93% coupled with a [FA] of 77 mM at − 1.6 V vs Ag/AgCl after 3 h. In addition, it was reported that the HER is likely to be suppressed using the Bi/C-NP based electrode with respect to the Bi rod, because of the larger double-layer contribution of the carbon substrate [47].

In this work, it was found that at 1 bar the nature of the cathode has a significant effect on the performance of the process. In particular, nanoparticle-based cathodes gave better results when high j and low P_{CO_2} are adopted. On the other hand, at higher P_{CO_2} (15 bar), the effect of the nature of the cathode becomes less important and the best results were achieved with simple and relatively cheap electrodes, such as Bi or Sn ones. Moreover, it was highlighted that all the cathodes tested in this work strongly benefit from the utilization of pressurised CO_2.

2. Materials and methods

2.1. Preparation and characterization of Sn/C-NP and Bi/C-NP electrodes

Sn/C-NPs and Bi/C-NPs have been synthesised using the methodology described in previous works [47,49,50] and carried out at ambient temperature-pressure conditions. Very briefly, $BiCl_3$ and $SnCl_2 \bullet 2\ H_2O$ were used as precursors and dissolved in N,N-Dimethylformamide (DMF) under magnetic stirring conditions. Then, polyvinylpyrrolidone (PVP) is added as protecting agent and stirred for 30 min. The reduction of precursors occurs by adding solid $NaBH_4$ as reducing agent. After complete reduction (about 10 min), Vulcan XC-72R carbon powder was aggregated to support the nanoparticles (nominal metal-carbon loading about 20 wt%) under magnetic and ultrasonic stirring. Subsequently, the nanoparticles were precipitated by adding acetone to the colloidal solution. For complete cleaning of samples, they were filtered and washed with an acetone-water mixture. Finally, the nanoparticles were dried overnight at 55 °C under vacuum conditions. The electrodes were manufacturing by the air-brushing technique. Firstly, a catalytic ink, composed of an 80:20 sample to Nafion ratio and diluted to 2 wt% in absolute ethanol, was prepared. Then, the ink was sprayed on a carbon paper (TGPH-90, QuinTech) at 90 °C to facilitate solvent evaporation. Taking into consideration the experimental metal-carbon loading of the samples (determined by ICP-OES measurements), the final catalytic loading of the electrodes was adjusted to be about 0.9–0.8 $mg_{Sn/C\ or\ Bi/C}$ cm^{-2}.

The physicochemical characterization of the Sn/C-NPs and Bi/C-NPs used in this work have been described in detail in previous contributions [47,50,51]. In brief, the samples are composed by 10 nm Sn and Bi nanoparticles well-dispersed on carbon. The experimental metal to

carbon loadings of the samples are 16 and 9 wt% corresponding to Bi/C-NPs and Sn/C-NPs, respectively. As discussed in ref. [50], the differences between the nominal and the experimental loadings of the samples have been attributed to the residual presence of DMF and PVP trapped in the porosity of the carbon Vulcan as well as to some partial dissolution of the metals during the extensive washing steps of the samples. In addition, XPS measurements have shown that Bi or Sn oxides are the main components of the Bi and Sn samples, respectively. This is expected due to the exposure of the samples to air. However, it is worth recalling that the CO_2 electrochemical reduction will take place at sufficiently negative potential to warranty that these Bi or Sn oxides were electrochemically reduced to metallic state [50].

The electrodes composed by the Sn/C-NPs and Bi/C-NPs were characterized by SEM/EDX and cyclic voltammetry (Fig. 1). The results have been also described in previous contributions [50].

2.2. Reagents and electrolysis

The electrolytic solution was constituted by bi-distilled water as solvent and 0.1 M Na_2SO_4 (Janssen Chimica) as supporting electrolyte (V = 0.050 L). The initial pH of the electrolyte solution was settled using H_2SO_4 (ASigma Aldrich) at pH 4 [35]. CO_2 (99.999% purity; supplied by Rivoira) was used for the electrolysis. Electrolyses were performed at P_{CO_2} of 1 and 15 bar. Prior to all the electrolyses, the solution was purged for 30 min by CO_2.

Electrolyses were performed by using an AISI316 stainless steel cell with a cylindrical geometry, described in detail in ref. [35], able to work at high pressure. Briefly, it was equipped with a gas inlet, a pressure

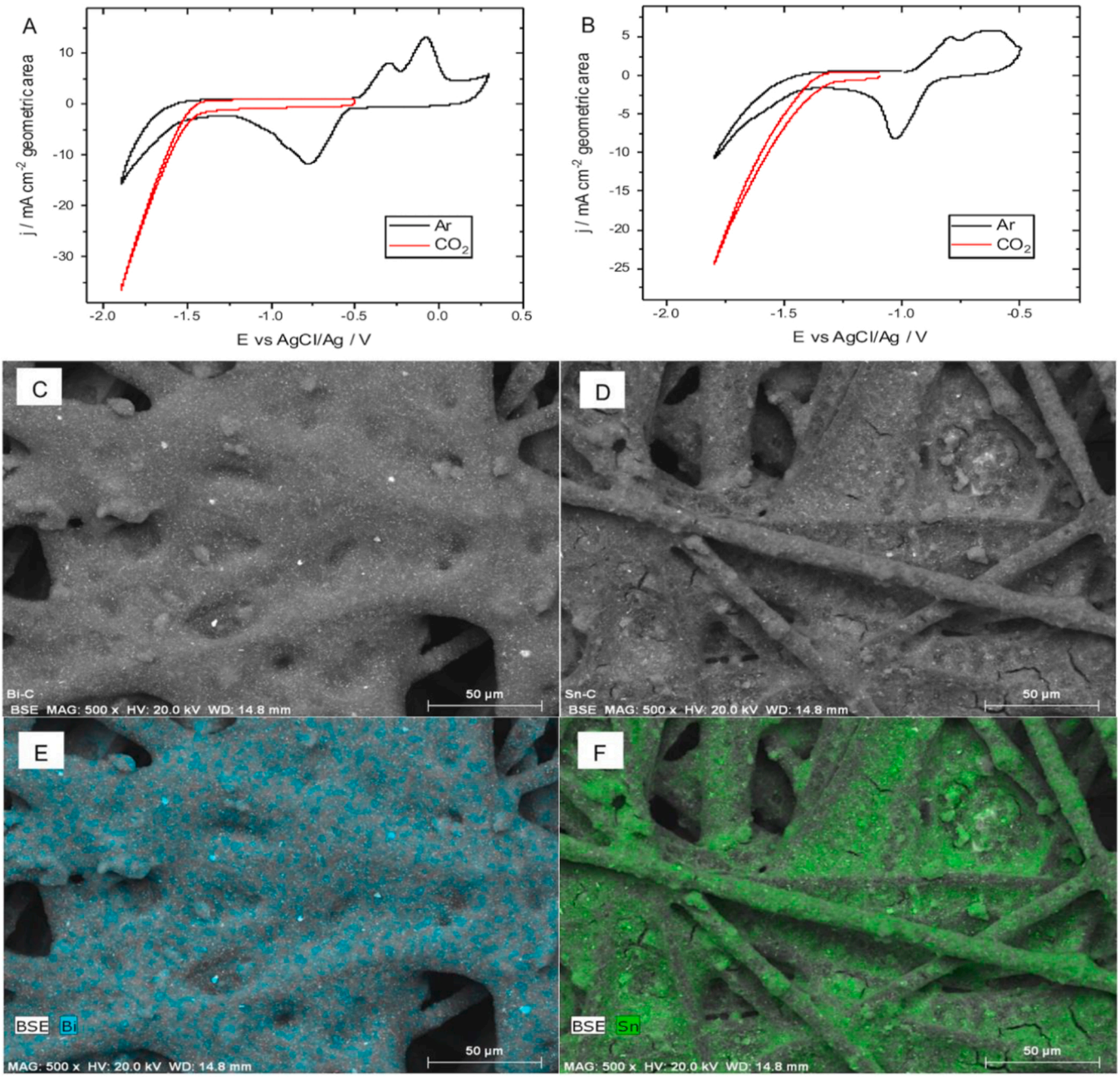

Fig. 1. Cyclic voltammetry characterization of the (A) Bi/C-NP and (B) Sn/C-NP electrodes in Ar (black line) and CO_2 (red line) saturated 0.45 M $KHCO_3$ and 0.5 M KCl aqueous electrolyte. Scan rate 50 mV s^{-1}. Catalyst loading of approximately 0.75 mg cm^{-2}. Field emission SEM images of the (C, E) Bi/C-NP and (D, F) Sn/C-NP electrode: coloured micrographs correspond to (C, D) SEM-EDX mapping and (E, F) the distribution of metal nanoparticles on the carbon substrate.

gauge, a dip tube connected to a pressure relief valve and two electrical line connections for the electrodes. The system worked with a continuous supply of carbon dioxide without accumulation of gases. CO_2 was used to pressurize the system at a flow of about 100 mL min^{-1} and the operative pressure was controlled using a pressure reducer. Electrolyses were performed in absence of stirring. The electrode gap was about 1 cm for both systems. Sn plate (metallic tin foil RPE, assay > 99%, supplied by Carlo Erba), Sn/C-NP, Bi rod and Bi/C-NP were selected as cathode materials; a Ti/IrO_2-Ta_2O_5 sheet anode (commercial DSA® from ElectroCell AB) was used as counter electrode. Sn plate was subjected to mechanically smoothing treatment, chemically pre-treated with a water solution of 11% HNO_3 (Romil Chemicals) for 2 min and, subsequently, cleaned with an ultrasound bath in distillate water for 5 min before each test. Bi rod cathode and DSA® anode were polished by ultrasound bath in bi-distillate water for 10 min. Nanoparticle-based electrodes were tested once and for each test replace with a new one.

Electrolyses were performed under galvanostatic condition (Amel 2053 potentiostat/galvanostat). To perform electrolyses at 10 °C, cooling was obtained using a tube wrapped around the reactor and connected to a chiller K20. The pump of the chiller allowed the circulation of the refrigerant liquid that was a water solution 33% v/v ethylene glycol. The thermal insulation was obtained covering the body of the reactor with a glass wool layer. Current density (j; mA/cm^2) was estimated as the ratio between the current intensity (I; A) and the cathodic wet geometrical-surface area (A; cm^2). A two-electrodes configuration was used in this system, with reference set on counter. Experiments were repeated at least twice with a reproducibility within 6% of the results. Electrolyses were carried out in absence of stirring of the solution.

2.3. Analytical methods

The performance of the process was discussed in terms of the following main figures of merit:

- Concentration of formic acid ([FA] [=] mM)
- Faradic efficiency (FE) (Eq. (1)) that measures the selectivity of the process towards a desired product, in the case of FA, and is defined as:

$$FE_{FA} = z * F * [FA]_t * V/(I * t) * 100\ [=]\ \% \quad (1)$$

where z is the number of electrons exchanged in the main reaction ($z = 2$ in the case of FA), F is the Faraday constant (96,485 C mol^{-1}), $[FA]_t$ is the FA concentration (mol L^{-1}) at the time t (s), V (L) is the volume of the solution.

- Energy consumption (EC) (Eq. (2)) and energy efficiency (EE) (Eq. (3)) are defined as:

$$EC = \Delta V * I * t/mol_{FA}\ [=]\ kWh\ mol^{-1} \quad (2)$$

$$EE = FE_{FA} * E_{eq}/\Delta V\ [=]\ \% \quad (3)$$

where ΔV is the cell potential, E_{eq} is the thermodynamic equilibrium cell potential (1.48 V for FA) and mol_{FA} the amount of FA obtained (mol).

The limiting current density, j_{lim} was computed as Eq. (4) [40]:

$$j_{lim}(T) = z * F * (\mathscr{D}_{CO_2}(T)/\delta) * c^b_{CO_2}(T)[=]mA\ cm^{-2} \quad (4)$$

where $\mathscr{D}_{CO_2}(T)$ is the CO_2 diffusion coefficient estimated at different T values [52], δ is the thickness of the stagnant layer and, at fixed P_{CO_2}, $c^b_{CO_2}(T)$ is the bulk CO_2 concentration. The $c^b_{CO_2}(T)$ was estimated according to the Henry's Law [32,52].

The thickness of the stagnant layer, δ, in absence of mixing rate was defined through a well-known diffusion limiting current technique using a very stable redox couple (i.e., Fe^{2+}/Fe^{3+}) [53,54]. The electrolytic solutions were constituted of aqueous solutions with the same concentrations of $K_4Fe(CN)_6$ thrihydrate 99% (Carlo Erba reagents) and $K_3Fe(CN)_6$ 99% (Merk) (20, 40 and 80 mM). The diffusion coefficient D values in water were assumed of 6.631 10^{-10} m^2 s^{-1} for this redox couple [53,54]. Hence, δ was evaluated using the following Eq. (5):

$$\delta = z * F * D * \partial c/\partial j_{lim}\ [=]\ m \quad (5)$$

where z is 1 for the Fe^{2+}/Fe^{3+} and $\partial c/\partial j_{lim}$is the experimental slope obtained plotting the concentrations of the used redox couple, i.e. 20, 40 and 80 mM, vs. the j_{lim} recorded by using a AutoLab PG- STAT12 at 0.005 V s^{-1} scan rate. According to these experimental procedures, it was estimated a δ of 100 μm.

To evaluate the [FA], Agilent HP 1100 HPLC fitted out with Rezex ROA-Organic Acid H+ (8%) column at 55 °C and coupled with a UV detector (210 nm) was used; 0.005 N H_2SO_4 water solution at pH 2.5 was eluted at 0.5 mL min^{-1} as mobile phase. The gas products were analized by gas cromathography using an Agilent 7890B GC fitted out with a Supelco Carboxen® 60/80 column and a thermal conductivity detector (TCD), working at 230 °C. Helium (99.999%, Air Liquide) at 1 bar was used as carrier gas. The temperature of the column was programmed, that is: an isotherm at 35 °C for 5 min followed by a 20 °C min^{-1} ramp up to 225 °C and by an isothermal step for 40 min

3. Results and discussion

3.1. Effect of the nature of the cathode at 1 bar

First electrolyses were performed for 3 h (194 C) using an aqueous electrolyte of 0.1 M Na_2SO_4, an initial pH of 4 and a gaseous current of CO_2 at 1 bar imposing a constant j of − 12 mA cm^{-2}. The undivided cell operated at 20 °C and was equipped with a Ti/IrO_2-Ta_2O_5 anode and four cathodes (Sn, Bi, Sn/C-NP, Bi/C-NP). The physicochemical characterization of the Sn/C-NPs and Bi/C-NPs used in this work have been described in detail in previous contributions (more detail in section *Materials and methods*) [47,50,51]. Using Sn electrode, the process allowed to synthesize FA with a final [FA] of 10.6 mM, a FE_{FA} close to 50% and an energetic consumption (EC) of 0.35 kWh mol^{-1} (Fig. 2). According to the literature [40], using Sn cathodes in aqueous electrolyte, the reduction of CO_2 to FA is expected to involve the following stages: (*i*) mass transfer of dissolved CO_2 to the cathode surface; (*ii*) adsorption of $CO_{2(aq)}$ (Eq. (6)); (*iii*) cathodic reduction of $CO_{2(ads)}$ to adsorbed $CO^-_{2(ads)}$• (Eq. (7)); (*iv*) cathodic reduction of $CO^-_{2(ads)}$• to FA (Eqs. (8) and (9)).

$$CO_{2(aq)} \rightleftharpoons CO_{2(ads)} \quad (6)$$

$$CO_{2(ads)} + e^- \rightleftharpoons CO^-_{2(ads)}\bullet \quad (7)$$

$$CO^-_{2(ads)}\bullet + H^+ \rightleftharpoons HCO_{2(ads)} \quad (8)$$

$$HCO_{2(ads)} + H^+ + e^- \rightleftharpoons HCOOH \quad (9)$$

Only a small amount of CO was obtained with a FE of CO close to 4%. Conversely, a significant production of hydrogen was detected, thus confirming that, using Sn electrodes, the synthesis of FA competes mainly with the water reduction to hydrogen (Eqs. (10) and (11) [40,41]:

$$H^+ + e^- \rightleftharpoons H_{(ads)} \quad (10)$$

$$H_{(ads)} + H^+ + e^- \rightleftharpoons H_2 \quad (11)$$

As shown in Fig. 2A, quite similar [FA] were achieved using Sn (10.6 mM) and Bi (10.2 mM) cathodes. Slightly higher and lower productions of FA were obtained using Bi/C-NP (11.80 mM) and Sn/C-NP (9.00 mM) cathodes, respectively (Fig. 2A). However, in all the cases, the FA was produced with a FE_{FA} lower than 60% (Fig. 2A), caused by a significant formation of hydrogen, and an EC higher than 0.30 kWh

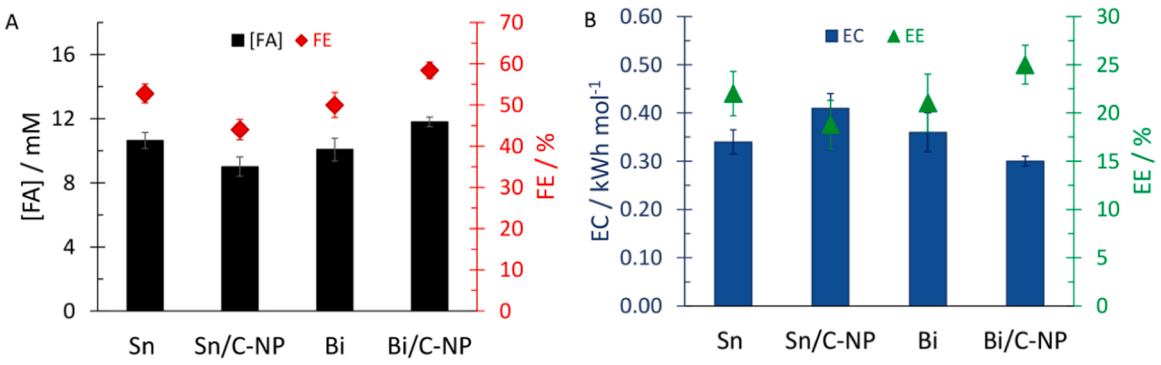

Fig. 2. Plot of the (A) [FA] and FE of FA and of (B) energetic consumption (EC) and energy efficiency (EE) for electrolyses carried out at under atmospheric P_{CO_2} using Sn, Sn/C-NP, Bi and Bi/C-NP electrodes. Electrolyses were performed under amperostatic condition j of − 12 mA cm^{-2} in CO_2 saturated 0.10 M Na_2SO_4 aqueous electrolyte (pH 4) for 3 h. $A_{cathode}$ = 1.50 cm^2. Counter: DSA® (Ti/IrO_2-Ta_2O_5 anode). V= 0.050 L.

mol^{-1} (Fig. 2B). As shown in Fig. 2B, the energy efficiency (EE) was between 19% and 25%. The best performances were obtained with Bi/C-NP cathode (FE_{FA} close to 60%, EE of 25% and EC of 0.30 kWh mol^{-1}).

It has been shown that the production of FA by CO_2EC requires, from an economic point of view, high productivities (e.g., high j coupled with high FE) and high [FA] to reduce the costs of concentration steps [7,8]. Hence, a series of electrolyses was performed at 1 bar using a higher j (j = −50 mA cm^{-2}) for the same amount of time passed (3 h), thus giving a higher charge passed (810 C) (Fig. 3). It is worth to mention that using Bi and Sn electrodes, a not drastic increase of the final [FA] was obtained with respect to the electrolyses performed at − 12 mA cm^{-2}, in spite of the higher amount of charge passed. As an example, using Bi cathode, higher j resulted in a very slight increase of the final [FA] from 10.10 to 11.20 mM (Figs. 2A and 3). This result is likely due to the fact that, under these relatively high j, using Bi, the process occurs under the kinetic control of the mass transfer of CO_2 to the cathode surface [40]. Indeed, the limiting current density (j_{lim}) is close to − 12 mA cm^{-2}. Hence, the production of FA cannot benefit of large j and charge passed adopted in these experiments that are used prevalently for the hydrogen evolution. For Sn, an even worse scenario is found. In this case, the increase of j from − 12 to − 50 mA cm^{-2} resulted in a significant decrease of the production of FA from 10.60 (FE close to 53%) to 7.80 mM (FE close to 9%) (Figs. 2A and 3). Indeed, in the case of Sn cathodes, it has been previously reported that at 1 bar, a relevant increase of the j and consequently of the working potential leads to a significant decrease of the selectivity of the process due to many probable causes [40]: (*i*) the H coverage is expected to increase, thus limiting the rate of CO_2 adsorption; (*ii*) the concentration of protons at the Sn surface is expected to decrease, thus reducing the rate of both Eqs. (8) and (9); (*iii*) the high H_2 evolution can cause a partial covering of the electrode surface by the gas bubbles, thus decreasing the rate of the mass transfer of CO_2 to the cathode.

As shown in Fig. 3, higher [FA] were obtained using carbon supported nanoparticles-based electrodes. As an example, when Sn cathode was replaced with Sn/C-NP electrode, the final [FA] increased from 7.80 to 11.10 mM. Similarly, the replacement of Bi with Bi/C-NP cathode, resulted in an increase of [FA] from 11.20 to 13.50 mM. According to previous works [50], the electroactive surface area of the nanoparticles-based electrodes is higher than that of corresponding plate ones. Hence, these results are probably due to the fact that nanoparticle-based electrodes present a higher active surface, thus giving higher j_{lim} and allowing to deal in a more effective way with higher j. However, in all the cases, the FE_{FA} (Fig. 3) and EE were quite low (< 5%), because of the massive oxidation of water to hydrogen.

3.2. *Effect of the nature of the cathode at 15 bar*

The effect of the nature of the cathode was evaluated also under pressurized conditions. Experiments were performed at 15 bar under amperostatic conditions j of − 12 or − 50 mA cm^{-2}. Quite interestingly, at − 12 mA cm^{-2}, the increase of the P_{CO_2} from 1 to 15 bar resulted in an increase of the production of FA and of the FE_{FA} for all tested electrodes. As shown in Figs. 2 and 4, the [FA] increased for Sn from 10.60 mM (FE_{FA} 53% and EE 22%) to 13.00 mM (FE_{FA} 65% and EE 27%) and for Bi from 10.10 mM (FE_{FA} 54% and EE 21%) to 15.60 mM (FE_{FA} 77% and EE 34%). Similarly, a significant improvement of the performances was achieved for nanoparticle-based cathodes (Figs. 2 and 4), thus confirming the positive effect of the P_{CO_2} on the conversion of CO_2 to FA previously observed using Sn cathodes [35,36]. Indeed, higher P_{CO_2} give rise to an increase of CO_2 solubility, thus accelerating its mass transfer to

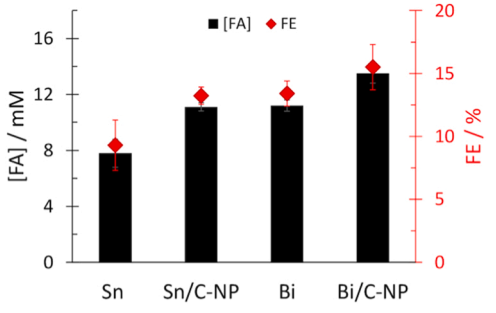

Fig. 3. Plot of the [FA] and FE of FA for electrolyses carried out at under atmospheric P_{CO_2} using Sn, Sn/C-NP, Bi and Bi/C-NP electrodes. Electrolyses were performed under amperostatic condition j of − 50 mA cm^{-2} in CO_2 saturated 0.10 M Na_2SO_4 aqueous electrolyte (pH 4) for 3 h. $A_{cathode}$ = 1.50 cm^2. Counter: DSA® (Ti/IrO_2-Ta_2O_5 anode). V= 0.050 L.

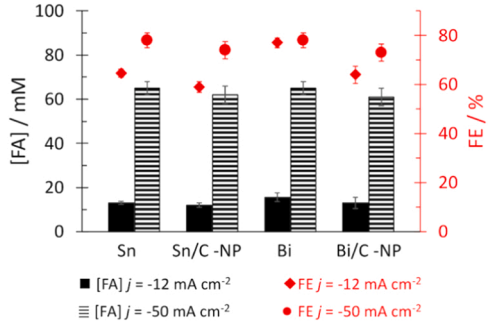

Fig. 4. Plot of the [FA] and FE of FA for electrolyses carried out under P_{CO_2} of 15 bar using Sn, Sn/C-NP, Bi and Bi/C-NP electrodes. Electrolyses were performed under amperostatic condition j of − 12 or − 50 mA cm^{-2} in CO_2 saturated 0.10 M Na_2SO_4 aqueous electrolyte (pH 4) for 3 h. $A_{cathode}$ = 1.50 cm^2. Counter: DSA® (Ti/IrO_2-Ta_2O_5 anode). V= 0.050 L.

the cathode surface and favouring both the adsorption step (Eq. (6)) and the successive reduction (Eq. (7)). At this *j* value, the best performances were achieved using Bi (Fig. 4) with an EC of 0.23 kWh mol^{-1} and an EE of 34%.

When the *j* was increased to − 50 mA cm^{-2}, the effect of the P_{CO_2} was even more remarkable. As shown in Fig. 4, the increase of the *j* coupled with the utilization of pressurized CO_2 allowed to enhance drastically the final [FA] maintaining good values of the FE_{FA}. As an example, using Sn based cathodes (Sn and Sn/C-NP) and P_{CO_2} of 15 bar, the [FA] was close to 12–13 and 62–65 mM at − 12 and − 50 mA cm^{-2}, respectively, after 3 h. Moreover, the FE_{FA} increased from 59–65% to 74–78% by increasing the j from − 12 to − 50 mA cm^{-2}, respectively. Similarly, using Bi based cathodes (Bi and Bi/C-NP), the [FA] was close to 13–16 mM (FE_{FA} = 59–65%) and 61 − 65 mM (FE_{FA} = 73–78%) at − 12 and − 50 mA cm^{-2}, respectively, after 3 h. It is worth to mention that, under these conditions, as shown in Fig. 4, very similar results were achieved at all adopted electrodes. Indeed, the final [FA] was observed to be between 61 and 65 mM with the four adopted cathodes.

It is worth to compare the results achieved at − 50 mA cm^{-2} under a P_{CO_2} of 1 and 15 bar. As shown in Figs. 3 and 4, the increase of the P_{CO_2} at this relatively high *j* allowed to increase both the production of FA and the FE_{FA}. As an example, using Sn, the [FA] increases of approximately 5 times (from 13 to 65 mM) in spite of the fact that the *j* was increased of about 4 times, because of the enhancement of the FE_{FA} from 65% to 78%. Similarly, the EC decreased from 2.91 to 0.32 kWh mol^{-1}.

3.3. Experiments performed at − 150 mA cm^{-2} and 15 bar

According to the literature, in order to develop the CO_2EC to FA on an applicative scale, it is mandatory to operate at high *j*, possibly higher than − 100 mA cm^{-2} [7,8]. Hence, a series of electrolyses was performed under amperostatic condition at a *j* value of − 150 mA cm^{-2} and 15 bar, using Sn, Bi, Sn/C-NP and Bi/C-NP cathodes. As shown in Fig. 5, the coupled utilization of relatively high *j* and P_{CO_2} allowed to increase drastically the production of FA with respect to that achieved with all the other operative conditions reported in the previous sections. Indeed, at all tested electrodes, a [FA] higher than 60 mM was achieved (Fig. 5). However, under these more severe conditions, a strong effect of the nature of the cathode was observed. In particular, the best results were obtained with Bi cathode that gave a [FA] slightly higher than 150 mM with a FE_{FA} higher than 60%. However, a relatively high EC (0.75 kWh mol^{-1}) was recorded mainly as a result of the higher cell potentials (ΔV) due to the high current intensities (*I* = - 225 mA). Quite good results were obtained also with Sn ([FA] close to 139 mM, FE_{FA} = 51%), while the nanoparticle-based electrodes presented a production of FA lower than 100 mM and a FE_{FA} lower than 40% (Fig. 5). In this framework, it is relevant to note that Ávila-Bolívar et al. [47] have evaluated the stability of the Bi-NPs for the CO_2 reduction into formate at − 1.6 V vs. Ag/AgCl

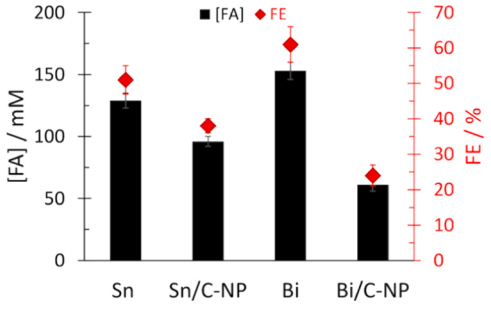

Fig. 5. Plot of the [FA] and FE of FA for electrolyses carried out under P_{CO_2} of 15 bar using Sn, Sn/C-NP, Bi and Bi/C-NP electrodes. Electrolyses were performed under amperostatic condition *j* of − 150 mA cm^{-2} in CO_2 saturated 0.10 M Na_2SO_4 aqueous electrolyte (pH 4) for 3 h. $A_{cathode}$ = 1.50 cm^2. Counter: DSA® (Ti/IrO_2-Ta_2O_5 anode). V= 0.050 L. Q = 2430 C.

for 24 h under atmospheric pressure. They have observed a decay trend of both the FE and the formate concentration starting after a passed charge of approximately 1620 C (*I* = 0.09 A; *t* = 5 h), which was mainly due to the loss of Bi during the electrolysis experiments. Hence, in our case, the worse performances given using nanoparticles-based cathodes could be attributed to the deactivation of the electrodes due to the loss on electrocatalysts during the electrolysis under the adopted conditions. Indeed, in our case, the total charge passed was approximately of 2430 C, which is much higher with respect to the starting degradation charge reported in literature (*Q* = 1620 C), thus resulting in a fast loss of process performances. Also, in these cases, the main competitive cathodic process was the HER.

3.4. Effect of the time passed

To evaluate the suitability of a cathode for the CO_2EC process, the stability of its performances with the time must be assessed. Hence, Sn and Bi cathodes were tested for about 30 h. In order to stress more the cathode, an electrode with a small surface (0.1 cm^2) was used. Experiments were performed at 10 °C and 10 bar using a CO_2 saturated 0.1 M Na_2SO_4 aqueous electrolyte at an initial pH of 4 and under amperostatic condition of − 75 mA cm^{-2}. As shown in Fig. 6, for both Sn and Bi, quite good results were achieved also for these long-run experiments. Indeed, using Sn, the [FA] increased almost linearly with the time passed with a final FE_{FA} close to 80%. In the case of Bi, even better results were achieved; a final FE_{FA} close to 90% was observed. To achieve other information of the stability of these electrodes, the same two Sn and Bi cathodes were used for some new electrolyses, under the same operative conditions, without any cleaning procedure between the tests. As shown in Fig. 6, quite good reproducibility was observed for both Sn and Bi cathodes in spite of the fact that the electrodes worked for two electrolyses performed 30 h each and for an overall 60 h without any cleaning procedure (1st time and 2nd time). Moreover, both the ΔV (3.5 V) and the EC (about 0.20 kWh mol^{-1}) were almost stable with time.

4. Conclusion

In this work, the simultaneous effect of P_{CO_2} and of the nature of cathode on the performances of CO_2EC process into FA in 0.1 M Na_2SO_4 aqueous electrolyte was investigated using an undivided cell, different *j* and Sn, Sn/C-NP, Bi and Bi/C-NP cathodes. It was found that the P_{CO_2} strongly affects the performances of the process. In particular, the increase of P_{CO_2} leads to higher productions of FA and to higher FE_{FA} for all the tested cathodes. This positive effect was more relevant for higher *j* values. As an example, at − 50 mA cm^{-2}, the increase of the P_{CO_2} allowed to increase the FE_{FA} of more than five times for most of tested cathodes. The effect of the nature of cathode is more complex:

- for low P_{CO_2} and intermediate values of *j* (1 bar and −50 mA cm^{-2}), the best performances were obtained with nanoparticle-based cathodes;
- for relatively high P_{CO_2} and intermediate values of *j* (15 bar and −50 mA cm^{-2}), very similar results were obtained with all the tested electrodes (([FA] = 59–65 mM and FE_{FA} = 73–78% after 3 h);
- for relatively high P_{CO_2} and higher *j* values (15 bar and −150 mA cm^{-2}), the best performances were obtained with simple Bi ([FA] = 151 mM and FE_{FA} = 61%) and Sn cathodes ([FA] = 139 mM and FE_{FA} = 51%).

Moreover, it was found that both Bi and Sn show quite good stable performances an overall period of 60 h.

CRediT authorship contribution statement

Federica Proietto: Investigation, Methodology, Data curation,

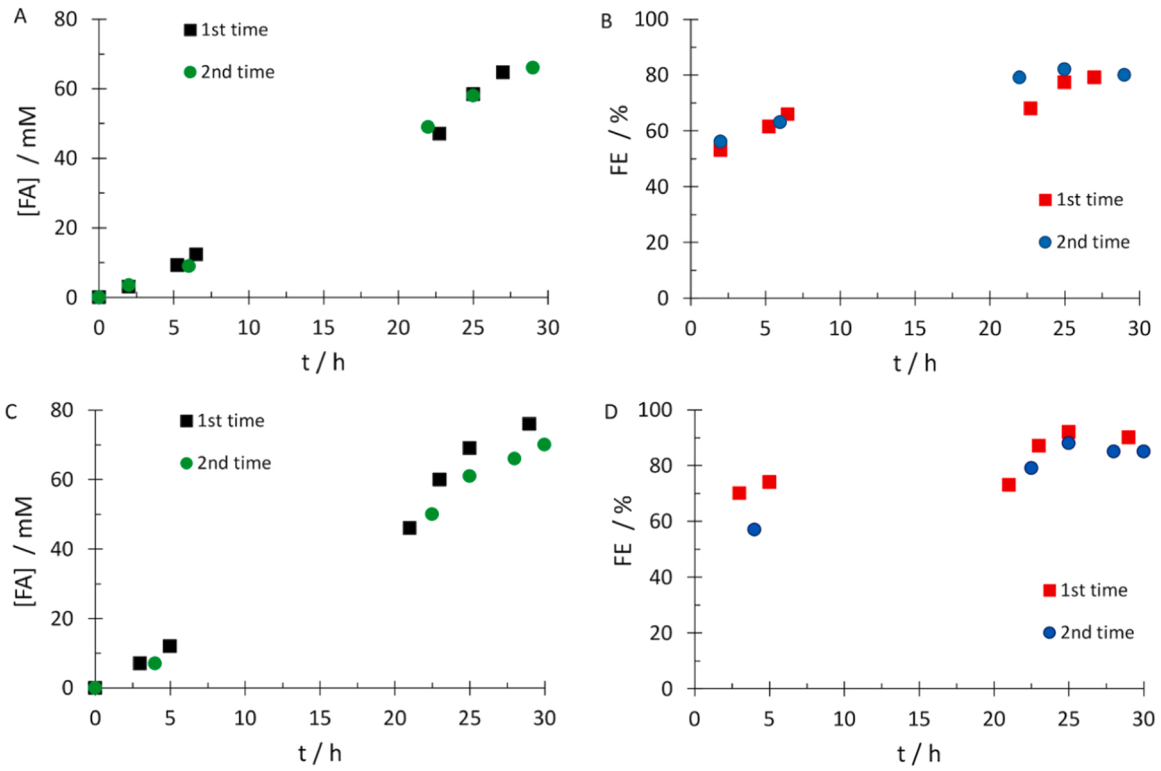

Fig. 6. Plot of the (A) [FA] and (B) FE of FA vs time passed using Sn cathode. Plot of the (C) [FA] and (D) FE of FA vs time passed using Bi cathode. Electrolyses were performed at 10 bar and 10 °C under amperostatic condition j of − 75 mA cm^{-2} in CO_2 saturated 0.10 M Na_2SO_4 aqueous electrolyte (pH 4) for 30 h. $A_{cathode}$ = 0.10 cm^2. Counter: DSA® (Ti/IrO_2-Ta_2O_5 anode). V= 0.050 L.

Writing – review & editing. **Riccardo Rinicella:** Investigation, Data curation. **Alessandro Galia**: Writing – review & editing, Funding acquisition. **Beatriz Ávila-Bolívar**: Investigation, Writing – review & editing. **Vicente Montiel**: Writing – review & editing, Funding acquisition. **José Solla-Gullón**: Writing – review & editing, Supervision, Funding acquisition. **Onofrio Scialdone**: Conceptualization, Methodology, Writing – review & editing, Supervision, Funding acquisition.

Declaration of Competing Interest

The authors declare that they have no known competing financial interests or personal relationships that could have appeared to influence the work reported in this paper.

Data availability

Data will be made available on request.

References

[1] W. Zhang, Y. Hu, L. Ma, G. Zhu, Y. Wang, X. Xue, Progress and perspective of electrocatalytic CO_2 reduction for renewable carbonaceous fuels and chemicals, Adv. Sci. 5 (2018), 1700275, https://doi.org/10.1002/advs.201700275.

[2] O.S. Bushuyev, P. De Luna, C.T. Dinh, L. Tao, G. Saur, J. Van De Lagemaat, S. O. Kelley, E.H. Sargent, What should we make with CO_2 and how can we make it? Joule 2 (2018) 825–832, https://doi.org/10.1016/j.joule.2017.09.003.

[3] P.R. Yaashikaa, P.S. Kumar, S.J. Varjani, A. Saravanan, A review on photochemical, biochemical and electrochemical transformation of CO_2 into value-added products, J. CO_2 Util. 33 (2019) 131–147, https://doi.org/10.1016/j.jcou.2019.05.017.

[4] F. Proietto, U. Patel, A. Galia, O. Scialdone, Electrochemical conversion of CO_2 to formic acid using a Sn based electrode: A critical review on the state-of-the-art technologies and their potential, Electrochim. Acta 389 (2021), 138753, https://doi.org/10.1016/j.electacta.2021.138753.

[5] M.F. Philips, G.J.M. Gutter, M.T.M. Koper, K.J.P. Schouten, Optimizing the electrochemical reduction of CO_2 to formate: a state-of-the-art analysis, ACS Sustain, Chem. Eng. 8 (2020) 15430–15444, https://doi.org/10.1021/acssuschemeng.0c05215.

[6] Y. Hori, H. Wakabe, T. Tsukamoto, O. Koga, Electrocatalytic process of CO selectively in electrochemical reduction of CO_2 at metal electrodes in aqueous media, Electrochim. Acta 39 (1994) 1833–1839, https://doi.org/10.1016/0013-4686(94)85172-7.

[7] Z. Huang, R.G. Grim, J.A. Schaidle, L. Tao, The economic outlook for converting CO_2 and electrons to molecules, Energy Environ. Sci. 14 (2021) 3664–3678, https://doi.org/10.1039/D0EE03525D.

[8] F. Proietto, A. Galia, O. Scialdone, Towards the Electrochemical Conversion of CO_2 to Formic Acid at an Applicative Scale: Technical and Economic Analysis of Most Promising Routes, ChemElectroChem 8 (2021) 2169–2179, https://doi.org/10.1002/celc.202100213.

[9] O. Scialdone, A. Galia, G. Errante, A.A. Isse, A. Gennaro, G. Filardo, Electrocarboxylation of benzyl chlorides at silver cathode at the preparative scale level, Electro Acta 53 (2008) 2514–2528, https://doi.org/10.1016/j.electacta.2007.10.021.

[10] O. Scialdone, A. Galia, A.A. Isse, A. Gennaro, M.A. Sabatino, R. Leone, G. Filardo, Electrocarboxylation of aromatic ketones: Influence of operative parameters on the competition between ketyl and ring carboxylation, J. Electroanal. Chem. 609 (2007) 8–16, https://doi.org/10.1016/j.jelechem.2007.02.014.

[11] M. Jouny, W. Luc, F. Jiao, General techno-economic analysis of CO_2 electrolysis systems, Ind. Eng. Chem. Res. 57 (2018) 2165–2177, https://doi.org/10.1021/acs.iecr.7b03514.

[12] S. Sabatino, A. Galia, G. Saracco, O. Scialdone, Development of an electrochemical process for the simultaneous treatment of wastewater and the conversion of carbon dioxide to higher value products, ChemElectroChem 4 (2017) 150–159, https://doi.org/10.1002/celc.20160 0475.

[13] T.E. Lister, E.J. Dufek, Chlor-syngas: coupling of electrochemical technologies for production of commodity chemicals, Energy Fuels 27 (2013) 4244–4249, https://doi.org/10.1021/ef302033j.

[14] P. Ma, X. Hao, F. Proietto, A. Galia, O. Scialdone, Assisted reverse electrodialysis for CO_2 electrochemical conversion and treatment of wastewater: A new approach towards more eco-friendly processes using salinity gradients, Electrochim. Acta 354 (2020), 136733, https://doi.org/10.1016/j.electacta.2020.136733.

[15] Y. Fu, Y. Li, X. Zhang, Y. Liu, J. Qiao, J. Zhang, D.P. Wilkinson, Novel hierarchical SnO_2 microsphere catalyst coated on gas diffusion electrode for enhancing energy efficiency of CO_2 reduction to formate fuel, Appl. Energy 175 (2016) 536–544, https://doi.org/10.1016/j.apenergy.2016.03.115.

[16] A. Del Castillo, M. Alvarez-Guerra, A. Irabien, Continuous electroreduction of CO_2 to formate using Sn gas diffusion electrodes, AIChE J. 60 (2014) 3557–3564, https://doi.org/10.1002/aic.14544.

[17] Q. Wang, H. Dong, H. Yu, Fabrication of a novel tin gas diffusion electrode for electrochemical reduction of carbon dioxide to formic acid, RSC Adv. 4 (2014) 59970–59976, https://doi.org/10.1039/C4RA10775F.

[18] Q. Wang, H. Dong, H. Yu, Development of rolling tin gas diffusion electrode for carbon dioxide electrochemical reduction to produce formate in aqueous electrolyte, J. Power Sources 271 (2014) 278–284, https://doi.org/10.1016/j.jpowsour.2014.08.017.
[19] J. Wu, F.G. Risalvato, P.P. Sharma, P.J. Pellechia, F.S. Ke, X.D. Zhou, Electrochemical reduction of carbon dioxide I. effects of the electrolyte on the selectivity and activity with Sn electrode, J. Electrochem. Soc. 160 (2013) F953–F957, https://doi.org/10.1149/2.049207jes.
[20] S. Guan, A. Agarwal, E. Rode, D. Hill, N. Sridhar, 3-D tin-carbon fiber paper electrodes for electrochemically converting CO_2 to formate/formic acid, Ceram. Trans. 241 (2013) 231–243, https://doi.org/10.1002/9781118751176.ch23.
[21] D. Kopljar, A. Inan, P. Vindayer, N. Wagner, E. Klemm, Electrochemical reduction of CO_2 to formate at high current density using gas diffusion electrodes, J. Appl. Electrochem 44 (2014) 1107–1116, https://doi.org/10.1007/s10800-014-0731-x.
[22] J. Wu, F.G. Risalvato, S. Ma, X. Zhou, Electrochemical reduction of carbon dioxide III. The role of oxide layer thickness on the performance of Sn electrode in a full electrochemical cell, J. Mater. Chem. A 2 (2014) 1647–1651, https://doi.org/10.1039/C3TA13544F.
[23] S. Lee, H. Ju, R. Machunda, S. Uhm, J.K. Lee, H.J. Lee, J. Lee, Sustainable production of formic acid by electrolytic reduction of gaseous carbon dioxide, J. Mater. Chem. A 3 (2015) 3029–3034, https://doi.org/10.1039/C4TA03893B.
[24] Q. Wang, H. Dong, H. Yu, H. Yu, Enhanced performance of gas diffusion electrode for electrochemical reduction of carbon dioxide to formate by adding polytetrafluoroethylene into catalyst layer, J. Power Sources 279 (2015) 1–5, https://doi.org/10.1016/j.jpowsour.2014.12.118.
[25] A. Del Castillo, M. Alvarez-Guerra, J. Solla-Gullón, A. Sáez, V. Montiel, A. Irabien, Electrocatalytic reduction of CO_2 to formate using particulate Sn electrodes: Effect of metal loading and particle size, Appl. Energy 157 (2015) 165–173, https://doi.org/10.1016/j.apenergy.2015.08.012.
[26] J. Wu, P.P. Sharma, B.H. Harris, X. Zhou, Electrochemical reduction of carbon dioxide: IV dependence of the Faradaic efficiency and current density on the microstructure and thickness of tin electrode, J. Power Sources 258 (2014) 189–194, https://doi.org/10.1016/j.jpowsour.2014.02.014.
[27] A. Del Castillo, M. Alvarez-Guerra, J. Solla-Gullon, A. Saez, V. Montiel, A. Irabien, Sn nanoparticles on gas diffusion electrodes: Synthesis, characterization and use for continuous CO_2 electroreduction to formate, J. CO_2 Util. 18 (2017) 222–228, https://doi.org/10.1016/j.jcou.2017.01.021.
[28] J.J. Kaczur, H. Yang, Z. Liu, S.D. Sajjad, R.I. Masel, Carbon dioxide and water electrolysis using new alkaline stable anion membranes, Front. Chem. 6 (2018) 263, https://doi.org/10.3389/fchem.2018.00263.
[29] G. Díaz-Sainz, M. Alvarez-Guerra, A. Irabien, Continuous Electrochemical Reduction of CO_2 to Formate: Comparative Study of the Influence of the Electrode Configuration with Sn and Bi-Based Electrocatalysts, Molecules 25 (2020) 4457, https://doi.org/10.3390/molecules25194457.
[30] G. Díaz-Sainz, M. Alvarez-Guerra, J. Solla-Gullón, L. García-Cruz, V. Montiel, A. Irabien, CO_2 electroreduction to formate: Continuous single-pass operation in a filter-press reactor at high current densities using Bi gas diffusion electrodes, J. CO_2 Util. 34 (2019) 12–19, https://doi.org/10.1016/j.jcou.2019.05.035.
[31] K. Hara, A. Kudo, T. Sakata, Electrochemical reduction of carbon dioxide under high pressure on various electrodes in an aqueous electrolyte, J. Electroanal. Chem. 391 (1995) 141–147, https://doi.org/10.1016/0022-0728(95)03935-A.
[32] A.R.T. Morrison, V. Van Beusekom, M. Ramdin, L.J.P. Van Den, T.J.H. Vlugt, W. De Jong, Modeling the electrochemical conversion of carbon dioxide to formic acid or formate at elevated pressures, J. Electrochem. Soc. 166 (2019) E77–E86, https://doi.org/10.1149/2.0121904jes.
[33] F. Köleli, T. Yesilkaynak, D. Balum, High pressure-high temperature CO_2 electro-reduction on Sn granules in a fixed-bed reactor, Fresenius Environ. Bull. 12 (2003) 1202–1206.
[34] F. Köleli, D. Balun, Reduction of CO_2 under high pressure and high temperature on Pb-granule electrodes in a fixed-bed reactor in aqueous medium, Appl. Catal. A Gen. 274 (2004) 237–242, https://doi.org/10.1016/j.apcata.2004.07.006.
[35] O. Scialdone, A. Galia, G. Lo Nero, F. Proietto, S. Sabatino, B. Schiavo, Electrochemical reduction of carbon dioxide to formic acid at a tin cathode in divided and undivided cells: effect of carbon dioxide pressure and other operating parameters, Electrochim. Acta 199 (2015) 332–341, https://doi.org/10.1016/j.electacta.2016.02.079.
[36] F. Proietto, B. Schiavo, A. Galia, O. Scialdone, Electrochemical conversion of CO_2 to HCOOH at tin cathode in a pressurized undivided filter-press cell, Electrochim. Acta 277 (2018) 30–40, https://doi.org/10.1016/j.electacta.2018.04.159.
[37] M. Ramdin, A.R.T. Morrison, M. De Groen, R. Van Haperen, R. De Kler, L.J.P. Van den Broeke, J.P.M. Trusler, W. De Jong, T.J.H. Vlugt, High pressure electrochemical reduction of CO_2 to formic acid/formate: a comparison between bipolar membranes and cation exchange membranes, Ind. Eng. Chem. Res. 58 (2019) 1834–1847, https://doi.org/10.1021/acs.iecr.8b04944.
[38] T. Mizuno, K. Ohta, A. Sasaki, T. Akai, M. Hirano, A. Kawabe, Effect of temperature on electrochemical reduction of high-pressure CO_2 with In, Sn, and Pb electrodes, Energy Sources 17 (5) (1995) 503–508, https://doi.org/10.1080/00908319508946098.
[39] E.J. Dufek, T.E. Lister, S.G. Stone, M.E. McIlwain, Operation of a Pressurized System for Continuous Reduction of CO_2, J. Electrochem. Soc. 159 (9) (2012) F514–F517, https://doi.org/10.1149/2.011209jes.
[40] F. Proietto, A. Galia, O. Scialdone, Electrochemical conversion of CO_2 to HCOOH at tin cathode: development of a theoretical model and comparison with experimental results, ChemElectroChem 6 (2019) 162–172, https://doi.org/10.1002/celc.201801067.
[41] O. Azizi, M. Jafarian, F. Gobal, H. Heli, M.G. Mahjani, The investigation of the kinetics and mechanism of hydrogen evolution reaction on tin, Int. J. Hydrog. Energy 32 (2007) 1755–1761, https://doi.org/10.1016/j.ijhydene.2006.08.043.
[42] K. Ito, T. Murata, S. Ikeda, Bulletin of Nagoya Institute of Technology, 1976: 209–214.
[43] S. Zhao, S. Li, T. Guo, S. Zhang, J. Wang, Y. Wu, Advances in Sn-Based Catalysts for Electrochemical CO_2 Reduction, Nano-Micro Lett. 11 (2019) 62, https://doi.org/10.1007/s40820-019-0293-x.
[44] S. Komatsu, T. Yanagihara, Y. Hiraga, M. Tanaka, A. Kunugi, Electrochemical reduction of CO_2 at Sb and Bi electrodes in KHCO3 solution, Denki Kagaku oyobi Kogyo Butsuri Kagaku 63 (3) (1995) 217–224, https://doi.org/10.5796/kogyobutsurikagaku.63.217.
[45] K. Fan, Y. Jia, Y. Ji, P. Kuang, B. Zhu, X. Liu, J. Yu, Curved surface boosts electrochemical CO_2 reduction to formate via bismuth nanotubes in a wide potential window, ACS Catal. 10 (2020) 358–364, https://doi.org/10.1021/acscatal.9b04516.
[46] A.S. Kumawat, A. Sarkar, Comparative study of carbon supported Pb, Bi and Sn catalysts for electroreduction of carbon dioxide in alkaline medium, J. Electrochem. Soc. 164 (2017) H1112, https://doi.org/10.1149/2.0991714jes.
[47] B. Ávila-Bolívar, L. García-Cruz, V. Montiel, J. Solla-Gullón, Electrochemical reduction of CO_2 to formate on easily prepared carbon-supported Bi nanoparticles, Molecules 24 (2019) 2032, https://doi.org/10.3390/molecules24112032.
[48] P. Su, W. Xu, Y. Qiu, T. Zhang, X. Li, H. Zhang, Ultrathin bismuth nanosheets as highly efficient electrocatalyst for CO_2 reduction, ChemSusChem 11 (2018) 848–853, https://doi.org/10.1002/cssc.201702229.
[49] A. Del Castillo, M. Alvarez-Guerra, J. Solla-Gullón, A. Sáez, V. Montiel, A. Irabien, Sn nanoparticles on gas diffusion electrodes: Synthesis, characterization and use for continuous CO_2 electroreduction to formate, J. CO_2 Util. 18 (2017) 222–228, https://doi.org/10.1016/j.jcou.2017.01.021.
[50] B. Ávila-Bolívar, V. Montiel, J. Solla-Gullón, Electrochemical Reduction of CO_2 to Formate on Nanoparticulated Bi−Sn−Sb Electrodes, ChemElectroChem 9 (2022), e202200272, https://doi.org/10.1002/celc.202200272.
[51] G. Díaz-Sainz, M. Alvarez-Guerra, B. Ávila-Bolívar, J. Solla-Gullón, V. Montiel, A. Irabien, Improving trade-offs in the figures of merit of gas-phase single-pass continuous CO_2 electrocatalytic reduction to formate, Chem. Eng. J. 405 (2021), 126965, https://doi.org/10.1016/j.cej.2020.126965.
[52] R. Perry, D. Green, Perry's Chemical Engineers' Handbook, 2008.
[53] A.A. Wragg, A.A. Leontaritis, Local mass transfer and current distribution in baffled and unbaffled parallel plate electrochemical reactors, Chem. Eng. J. 66 (1997) 1–10, https://doi.org/10.1016/S1385-8947(96)03148-8.
[54] C.A. Martínez-Huitle, S. Ferro, A. De Battisti, Electrochemical incineration of oxalic acid: Reactivity and engineering parameters, J. Appl. Electrochem. 35 (2005) 1087–1093, https://doi.org/10.1007/s10800-005-9003-0.